SEISMIC-HAZARD SCENARIO FOR AN M 7 EARTHQUAKE ALONG THE SALT LAKE CITY SEGMENT OF THE WASATCH FAULT ZONE, UTAH

Grant Award No. 99HQGR0091

Barry J. Solomon, Greg McDonald, Francis Ashland
Utah Geological Survey
P.O. Box 146100, Salt Lake City, Utah 84114-6100
Telephone: (801) 537-3388, FAX: (801) 537-3400
nrugs.bsolomon@state.ut.us, www.ugs.state.ut.us

Ivan Wong, Douglas Wright, Susan Olig
URS Corporation
500 12th Street, Suite 200, Oakland, California 94607
Telephone: (510) 874-3014, FAX: (510) 874-3268
Ivan_Wong@urscorp.com

Walter Silva, Nick Gregor
Pacific Engineering & Analysis
311 Pomona Avenue, El Cerrito, California 94530
Telephone: (510) 528-2821, FAX: (510) 528-2135
pacificengineering@juno.com, www.pacificengineering.org

NEHRP Element: I

Key Words: Regional Seismic Hazards, Strong Ground Motion, Earthquake Effects, Earthquake Scenarios

SCOPE OF INVESTIGATIONS

The Wasatch fault zone, one of the longest and most active normal-slip faults in the world, parallels the densely populated Wasatch Front area of Utah. The Salt Lake City segment, extending for about 46 kilometers, is one of the more active segments of the Wasatch fault zone (figure 1). This segment generated four surface-faulting earthquakes in the past 6,000 years (Black and others, 1996). A conservative estimate for the magnitude of a surface-faulting earthquake on the segment is moment magnitude (**M**) 7. A large earthquake within the Wasatch Front region would place more than 1.7 million people (2000 census) at risk and cause large losses to personal property and infrastructure.

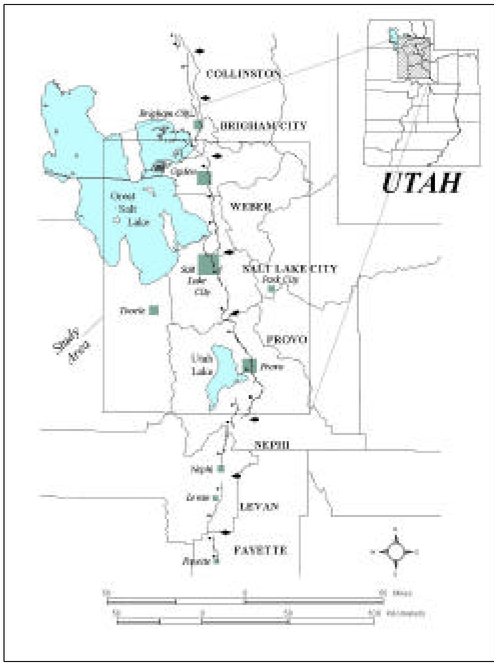

Emergency managers and planners need an accurate and current scenario of expected geologic effects that will likely occur during a large earthquake. We will take advantage of recent progress in geologic-hazard mapping of the Salt Lake City metropolitan area to analyze and map seismic hazards in a 16,000 square kilometer portion of the Wasatch Front resulting from an **M** 7 event along the Salt Lake City segment of the Wasatch fault zone. Our seismic-hazard maps, at a scale of 1:250,000, will be the basis for developing a scenario that can be used to estimate losses using risk-assessment methods developed jointly by the Federal Emergency Management Agency (FEMA) and the National Institute of Building Sciences, referred to as HAZUS (National Institute of Building Sciences, 1999). Our earthquake-scenario maps for ground shaking are complete. We will modify techniques used by HAZUS to map liquefaction, landsliding, and surface fault rupture hazards; use published estimates for tectonic subsidence; and estimate the potential for dam failure and seiches in Great Salt Lake.

Figure 1. *Outline of the study area and segments of the Wasatch fault zone with arrows showing segment boundaries.*

RESULTS OF COMPLETED STUDIES AND PROPOSED TECHNIQUES FOR FUTURE INVESTIGATIONS

Ground Shaking

To incorporate site-response effects into our computed ground motions, we modified site-response units defined by Ashland (2001) from surficial-geologic mapping and shear-wave velocity data for the Salt Lake Valley. We identified four site-response units, each divided into six thickness ranges with a maximum thickness of 488 meters of unconsolidated sediment, for a total of 24 subcategories. We used the stochastic numerical ground-motion modeling approach coupled with an equivalent linear methodology (Silva and others, 1998) to calculate amplification factors for 5 percent damped response spectra for each site-response unit. At peak horizontal acceleration, the median amplification factors ranged from 0.62 to 2.09 (values less than 1.0 signify deamplification). At 0.2 and 1.0-second spectral accelerations, the median factors ranged from 0.50 to 2.19 and 0.94 to 3.13, respectively.

We used empirical attenuation relations appropriate for soft rock sites in the western U.S. (Abrahamson and Silva, 1997; Campbell, 1997; Sadigh and others, 1997; Spudich and others, 1999) and numerical modeling to compute ground motions for the scenario earthquake. The relations were respectively weighted 0.40, 0.15, 0.15, and 0.30 to give the greatest weight to the two relations most appropriate for extensional regimes. Scenario ground-motion values were calculated by assigning a 0.40 weight to the values computed from the empirical attenuation relations and a 0.60 weight to the numerically modeled values. Our ground-motion maps show that high-frequency motions, characterized by peak horizontal acceleration, could approach or possibly exceed 1 *g* from the scenario earthquake. The highest ground motions (greater than 0.7 *g*) occur in stiff gravels and sands near the Wasatch fault, whereas lower ground motions occur over lacustrine and alluvial silts and clays that are damping out the high-frequency ground motions. Site effects appear to be more dominant than the hanging-wall effect.

Damaging ground shaking (greater than 0.1 *g*) will occur beyond Salt Lake Valley and will include the cities of Ogden and Provo along the Wasatch Front, Tooele to the west, and the back valleys of the Wasatch Range to the east. The pattern of ground shaking at short periods (0.2-second spectral acceleration) resembles that for peak acceleration. In contrast, the correspondence between site-response units and ground motions is not as strong for ground shaking at long periods (1.0-second spectral acceleration). At long periods, the highest ground motions (greater than 1.1 *g*) occur in the deeper portions of the basins having thick deposits of unconsolidated sediment. Directivity effects, which are long period in nature (greater than 0.5 seconds), are not readily apparent because they have been diluted somewhat by the use of empirical attenuation relations and/or masked by site effects.

Liquefaction

HAZUS maps liquefaction susceptibility using the classification system of Youd and Perkins (1978), which assigns a relative liquefaction susceptibility rating based on age, depositional environment, and material type. However, Anderson and others (1986) argue that the criteria of Youd and Perkins (1978) were defined for deposits in California and are not relevant to Utah's closed basins. Therefore, we will use liquefaction potential maps from Wasatch Front liquefaction studies (for example Anderson and others, 1986) and information on topographic and geologic settings to evaluate the liquefaction hazard in our study area. We will then calculate liquefaction probability using the HAZUS relation between conditional liquefaction probability (Liao and others, 1988), earthquake magnitude and ground-water depth (National Research Council, 1985), and the proportion of map units susceptible to liquefaction (which HAZUS determines from examination of soil-property data from various regional liquefaction studies such as Power and others [1982]).

We will use HAZUS techniques to estimate the amount of liquefaction-induced ground deformation related to each susceptibility category for both lateral spreading and ground settlement. For lateral spreading, HAZUS estimates ground deformation for each susceptibility category by combining the Liquefaction Severity Index relation of Youd and Perkins (1978) with the ground-motion attenuation relation of Sadigh and others (1986). The expected permanent ground displacement due to lateral spreading depends on the threshold ground acceleration necessary to induce liquefaction, which we will obtain using the critical accelerations from Wasatch Front liquefaction studies. We will then compare our mapped PGA to the threshold ground acceleration to determine the amount of permanent ground displacement. Because the relations to calculate displacement are based on an earthquake with M=7.5, we can adjust the calculation using a displacement correction factor, calculated by HAZUS based on work done by Seed and Idriss (1982). For ground settlement, HAZUS indicates that relations presented by Tokimatsu and Seed (1987) demonstrate very little dependence on ground-motion level given the occurrence of liquefaction. Therefore, HAZUS calculates the expected settlement for each susceptibility category as the product of the probability of liquefaction for a given ground-motion level and the characteristic settlement amplitude appropriate to the susceptibility category.

Landsliding

HAZUS uses the relation between critical acceleration, slope inclination, lithology, and ground-water depth developed by Wilson and Keefer (1985) as the basis for mapping landslide susceptibility. Wilson and Keefer (1985) define three geologic groups containing rock and soil having similar shear strengths. The landslide susceptibility of each group is divided into categories based on slope angle, and each category is defined as a function of critical acceleration. Landslide susceptibility is assigned to the categories for each of two conditions, wet (ground-water level at ground surface) and dry (ground water below level of sliding). We will use these relations to map landslide susceptibility by assigning each geologic unit from the statewide geologic map (Hintze, 1980) to a geologic group, subdividing the groups into categories based on slope using USGS Digital Elevation Models, and determining susceptibility under both wet and dry conditions to assure a complete estimate of landslide susceptibility.

Wieczorek and others (1985) indicate that the relations developed by Wilson and Keefer (1985) are conservative, representing the most landslide-susceptible geologic types likely to be found in each geologic group. The probability of slope failure must be considered when using these relations. HAZUS assesses the percentage of a landslide susceptibility category expected to be susceptible to landsliding using information from Wieczorek and others (1985). At any given location there is a specified probability of the presence of susceptible deposits depending on whether the induced PGA (determined from our map) exceeds the critical acceleration.

HAZUS calculates ground deformations due to landsliding using the approach developed by Newmark (1965). According to this approach, earthquake-induced downslope deformations occur when the induced PGA within the slide mass exceeds the critical acceleration, and the amount of downslope movement depends on the duration or number of cycles of ground shaking. Rather than using the Newmark method employed by HAZUS, we will use the modified Newmark method suggested by Jibson (1993) and updated by Jibson and others (1998) using data collected during and after the 1994 Northridge earthquake. This modified Newmark method establishes an empirical relation between Arias intensity, critical acceleration, and Newmark displacement. We can determine Arias intensity from two equations presented by Jibson (1993). Combining the two equations creates a third relation that permits us to calculate Arias intensity from PGA and earthquake moment magnitude. Wilson and Keefer (1985) define critical acceleration for each susceptibility category.

Surface Fault Rupture

We will use the method employed by HAZUS to estimate the hazard from surface fault rupture. This method is based on the empirical relation developed by Wells and Coppersmith (1994) between surface fault displacement and earthquake moment magnitude, and a probability distribution for values of displacement along the fault trace. The method assumes that the maximum displacement can potentially occur at any location along the fault, although displacements must drop to zero at the ends of the fault. However, considerable uncertainty exists in the maximum displacement—displacement estimates vary by a factor of two within plus-or-minus one standard deviation from the median estimate. For this reason, HAZUS conservatively estimates the probability distribution for values of displacement along the fault rupture segment. Wells and Coppersmith (1994) found that the average displacement along the fault rupture segment was approximately equal to one-half the maximum displacement. This is equivalent to a uniform probability distribution for values of displacement ranging from zero to the maximum displacement. As a conservative estimate, HAZUS incorporates a uniform probability distribution equivalent to average displacement ranging from a minimum of one-half of the maximum fault displacement (rather than zero) in the loss estimation methodology for any location along the fault rupture.

Tectonic Subsidence

Valley bottoms may tilt toward the Wasatch fault zone on the downdropped side of the surface fault rupture during a large earthquake. As a result, areas along the shores of Great Salt Lake may permanently subside, causing local flooding. Keaton (1986) mapped the inundation potential along the shores of Great Salt Lake for various probable lake levels during the next 100 years. Chang and Smith (1998) mapped the inundation potential by subtracting earthquake-induced topographic changes from ground elevations to determine the tectonic subsidence and new lake-shoreline locations. We will use these maps for our earthquake scenario. Subsidence may also cause a relative rise in ground-water levels, causing water to pond, and flooding basements and buried facilities. Keaton (1986) mapped areas of possible shallow ground-water flooding from tectonic subsidence, and we will use this map as well.

Dam-Failure Inundation

HAZUS includes information on 247 dams within our study area from a database developed from the National Inventory of Dams (FEMA, 1993). In the event of failure, many of these dams (high-hazard dams) may pose a threat to human life. However, the U.S. Bureau of Reclamation, U.S. Army Corps of Engineers, and Utah Division of Water Rights have dam-safety programs to evaluate the expected performance of large, high-hazard dams during earthquakes. If these dams were not initially designed and constructed to withstand large earthquakes, the programs require modification to provide better performance. Some of the modifications are complete and completion of the remainder is expected in the next few years. Once completed, officials believe all large, high-hazard dams in our study area will provide satisfactory performance with no uncontrolled releases during our scenario earthquake. Smaller high-hazard dams, including debris basins and flood-control structures, are not subject to seismic criteria but are generally dry and unlikely to contain significant amounts of water during the scenario. Thus, our scenario does not include dam-failure flooding.

Seiche

Few studies of seiche potential exist for lakes and reservoirs within our study area and seiche analysis for most of them is beyond the scope of our study. However, considerable interest exists in the seiche potential for Great Salt Lake because it lies near the Salt Lake City metropolitan area. Pechmann (1987) first discussed possible seiches in Great Salt Lake in an analysis of earthquake design considerations for the inter-island diking project. He noted that accounts of the 1909 M 6 Hansel Valley earthquake near the north lake shore reported significant earthquake-induced waves, which Lowe (1993) later estimated to be more than 3.7 meters high. These accounts suggested to Pechmann that the earthquake epicenter, although placed by felt reports about 15 kilometers north of the lake shore, might actually have occurred beneath the lake resulting in lake waves caused by displacement of the lake bottom rather than by ground shaking. The 1934 M 6.6 Hansel Valley earthquake did not generate similar lake waves, consistent with instrumental location of its epicenter and with surface faulting located just northeast of the north lake shore. Because our scenario earthquake does not involve lakebed displacement, this mechanism will not contribute to seiches in Great Salt Lake.

For generation of significant seiche waves by ground shaking, the frequency of earthquake ground motion must be close to the natural frequency of the lake. Lin and Wang (1978) determined that the fundamental mode of the natural period (the inverse of frequency) in the south basin of Great Salt Lake (the part of the lake nearest the Salt Lake City segment of the Wasatch fault zone) is 6.33 hours. However, the period of surface waves from strong earthquake ground motions is from about 15 to 25 seconds, and the period of body waves is even smaller. Because the frequency of strong earthquake ground motions is not close to the natural frequency of Great Salt Lake, seiche waves generated by ground shaking in our scenario earthquake will not be significant and will probably have a maximum wave height of only a few centimeters.

NON-TECHNICAL SUMMARY

A large earthquake on the active Wasatch fault zone may impact more than 1.7 million people living along the densely populated and rapidly expanding Wasatch Front urban area of northern Utah. We are studying earthquake hazards such as ground shaking, liquefaction, landsliding, surface fault rupture, tectonic subsidence, dam-failure inundation, and seiches resulting from a large earthquake on this fault zone near Salt Lake City. The study results will be used for emergency-response planning to identify potential earthquake effects and to estimate losses using risk-assessment methodology (HAZUS)

developed by the National Institute of Building Sciences for the Federal Emergency Management Agency.

REPORTS PUBLISHED

No reports have been published yet. Upon project completion, the Utah Geological Survey will publish the hazard maps and mapping protocols.

AVAILABILITY OF DATA

When complete, the seismic-hazard maps will be available in digital form through the Utah Geological Survey. The digitized maps will also be available from the State Geographic Information Database through the Utah Automated Geographic Reference Center.

REFERENCES

Abrahamson, N.A., and Silva, W.J., 1997, Empirical response spectral attenuation relations for shallow crustal earthquakes: Seismological Research Letters, v. 68, p. 94-127.

Anderson, L.R., Keaton, J.R., Spitzley, J.E., and Allen, A.C., 1986, Liquefaction potential map for Salt Lake County, Utah: Logan, Utah State University Department of Civil and Environmental Engineering and Dames and Moore unpublished Final Technical Report for the U.S. Geological Survey, 48 p.; published as Utah Geological Survey Contract Report 94-9, 1994.

Ashland, F.X., 2001, Site-response characterization for implementing ShakeMap in northern Utah: Utah Geological Survey Report of Investigation 248, 10 p.

Black, B.D., Lund, W.R., Schwartz, D.P., Gill, H.E., and Mayes, B.H., 1996, Paleoseismic investigation on the Salt Lake City segment of the Wasatch fault zone at the South Fork Dry Creek and Dry Gulch sites, Salt Lake County, Utah: Utah Geological Survey Special Study 92, 22 p.

Campbell, K.W., 1997, Empirical near-source attenuation relationships for horizontal and vertical components of peak ground acceleration, peak ground velocity, and pseudo-absolute acceleration response spectra: Seismological Research Letters, v. 68, p. 154-179.

Chang, W.L., and Smith, R.B., 1998, Potential for tectonically induced tilting and flooding by the Great Salt Lake, Utah, from large earthquakes on the Wasatch fault, *in* Lund, W.R., Proceedings volume—Basin and Range Province seismic-hazards summit: Utah Geological Survey Miscellaneous Publication 98-2.

Federal Emergency Management Agency, 1993, Water control infrastructure, national inventory of dams 1992: Washington, D.C., Federal Emergency Management Agency and U.S. Army Corps of Engineers.

Hintze, L.F., 1980, Geologic map of Utah: Utah Geological Survey Map A-1, scale 1:500,000.

Jibson, R.W., 1993, Predicting earthquake-induced landslide displacements using Newmark's sliding block analysis: Transportation Research Record, no. 1411, p. 9-17.

Jibson, R.W., Harp, E.L., and Michael, J.A., 1998, A method for producing digital probabilistic seismic landslide hazard maps—an example from the Los Angeles, California, area: U.S. Geological Survey Open-File Report 98-113, 17 p.

Keaton, J.R., 1986, Potential consequences of tectonic deformation along the Wasatch fault: Logan, Utah State University, Department of Civil and Environmental Engineering unpublished Final Technical Report for the U.S. Geological Survey, 23 p.

Liao, S.S., Veneziano, D., and Whitman, R.V., 1988, Regression models for evaluating liquefaction probability: Journal of Geotechnical Engineering, v. 114, no. 4.

Lin, Anching, and Wang, Po, 1978, Wind tides of the Great Salt Lake: Utah Geology, v. 5, no. 1, p. 17-25.

Lowe, Mike, 1993, Hazards from earthquake-induced ground failure in sensitive clays, vibratory settlement, and flooding due to seiches, surface-drainage disruptions, and increased ground-water discharge, Davis County, Utah, *in* Gori, P.L., editor, Applications of research from the U.S. Geological Survey program, Assessment of Regional Earthquake Hazards and Risk Along the Wasatch Front, Utah: U.S. Geological Survey Professional Paper 1519, p. 163-167.

National Institute of Building Sciences, 1999, Earthquake loss estimation methodology—HAZUS user's manual: Washington, D.C., Federal Emergency Management Agency, 11 chapters and 8 appendices.

National Research Council, 1985, Liquefaction of soils during earthquakes: Washington, D.C., Committee on Earthquake Engineering, Commission on Engineering and Technical Systems, National Academy Press.

Newmark, N.M., 1965, Effects of earthquakes on dams and embankments: Geotechnique, v. 15, p. 139-160.

Pechmann, J.C., 1987, Earthquake design considerations for the inter-island diking project, Great Salt Lake, Utah: Salt Lake City, unpublished technical report for Rollins, Brown, and Gunnell, Inc., 31 p.

Power, M.S., Dawson, A.W., Streiff, D.W., Perman, R.G., and Haley, S.C., 1982, Evaluation of liquefaction susceptibility in the San Diego, California urban area: Proceedings of the 3rd International Conference on Microzonation, v. II, p. 957-968.

Sadigh, K., Chang, C.-Y., Egan, J.A., Makdisi, F., and Youngs, R.R., 1997, Attenuation relationships for shallow crustal earthquakes based on California strong motion data: Seismological Research Letters, v. 68, p. 180-189.

Sadigh, K., Egan, J.A., and Youngs, R.R., 1986, Specification of ground motions for seismic design on long period structures: Earthquake Notes, v. 57, no. 1, p. 13.

Seed, H.B., and Idriss, I.M., 1982, Ground motions and soil liquefaction during earthquakes: Oakland, California, Earthquake Engineering Research Institute, Monograph Series, p. 13.

Silva, W.J., Wong, I.G., and Darragh, R.B., 1998, Engineering characterization of earthquake strong ground motions in the Pacific Northwest, *in* Rogers, A.M., Walsh, T.J., Kockelman, W.J., and Priest, G.R., editors, Assessing earthquake hazards and reducing risk in the Pacific Northwest: U.S. Geological Survey Professional Paper 1560, v. 2, p. 313-324.

Spudich, P., Joyner, W.B., Lindh, A.G., Boore, D.M., Margaris, B.M., and Fletcher, J.B., 1999, SEA99—A revised ground motion prediction relation for use in extensional tectonic regimes: Bulletin of the Seismological Society of America, v. 89, p. 1,156-1,170.

Tokimatsu, A.M., and Seed, H.B., 1987, Evaluation of settlements in sand due to earthquake shaking: Journal of the Geotechnical Engineering Division, American Society of Civil Engineers, v. 113, no. 8.

Wells, D.L., and Coppersmith, K.J., 1994, New empirical relationships among magnitude, rupture length, rupture width, and surface displacement: Bulletin of the Seismological Society of America, v. 84.

Wieczorek, G.F., Wilson, R.C., and Harp, E.L., 1985, Map of slope stability during earthquakes in San Mateo County, California: U.S. Geological Survey Miscellaneous Investigations Map I-1257E, scale 1:62,500.

Wilson, R.C., and Keefer, D.K., 1985, Predicting areal limits of earthquake-induced landsliding, *in* Ziony, J.I., editor, Evaluating earthquake hazards in the Los Angeles region--an earth-science perspective: U.S. Geological Survey Professional Paper 1360, p. 317-345.

Youd, T.L., and Perkins, D.M., 1978, Mapping liquefaction-induced ground failure potential: Journal of the Geotechnical Engineering Division, American Society of Civil Engineers, v. 104, p. 433-446.